Table 4 Effect of specific form of aluminum fuel on the propellant burning rate

Aluminum form	Range of burning-rate increase, %
Hollow sphere	50–100
Hollow tubes	10–200
Staple	20–300
Wire	50–400
Foil	50–450
Reactive metal coating	100–1100

Table 5 Effect of metal wire on burning rate (reference rate is 0.50 in./sec)

Wire used			
Metal	α[a], cm²/sec	m.p., °C	r, along wire in./sec
Ag	1.23	960	2.65
Cu	0.90	1083	2.32
W	0.67	3370	1.82
Pt	0.35	1755	1.46
Al	0.94	660	1.16
Mg[b]	0.66	651	0.96
Steel[c]	0.064	1460 est.	0.80

[a] Thermal diffusivity at 650 C.
[b] Square filament cut from 0.005-in. Mg sheet.
[c] Music wire.

Table 6 Typical propellant development cycle

Cycle step	Time period, month
Establish propellant ballistic requirements	1–2
Analytical studies to define propellant formulation	1–2
Laboratory formulation	2–6
Small motor testing	3–6
Intermediate-scale motor testing	3–8
Full-size motor testing	6–8
Total months (does not include the time necessary to synthesize any of the ingredients)	16–42

lation and curing techniques, physical properties, and handling, storage, and safety properties of the propellants must be carefully evaluated, of course.

It is estimated (Table 6) that if a variable-burning-rate propellant were available, a typical propellant development cycle would be reduced by 16 to 42 months, depending upon the amount of motor testing required for acceptance. The monetary savings might be on the order of 1–3 million dollars. Furthermore, special facilities are often required for the production of the necessary raw materials for new multiple-ingredient propellants, and these facilities are often shut down at the end of the program. If the large effort now being expended on the development of a multitude of propellants could be transferred to the cause of increasing the knowledge about a few variable-burning-rate systems, a great savings in future program times and costs should result.

References

[1] Vandenkerckhove, J., "Comment on 'A practical approach to grain design,'" Jet Propulsion **28**, 766–768 (1958).

[2] Stone, M. W., "Slotted tube grain design," ARS J. **31**, 223 (1961).

[3] Price, E. W., "Change geometry and ballistic parameters for solid propellant rocket motors," Jet Propulsion **24**, 16–21 (1954).

[4] "Increasing the performance of solid propellant grains through the use of metal heat conductors," Atlantic Research Corp. (July 1963).

Influences of Small Differences in Ballistic Coefficient on Satellite Station Keeping

SHIH-YUAN CHEN*
The Rand Corporation, Santa Monica, Calif.

Nomenclature

g_E = earth's gravity
h = altitude
h_0 = satellite initial altitude at $t = 0$
h_1 = $R_1 - R_E$ = satellite altitude at the end of time t
n = integer
R = radius
R_0 = $R_E + h_0$
R_E = earth's radius
t = elapsed time
β = ballistic coefficient
γ = reciprocal of scale height
θ = anomaly angle
ρ = atmospheric density
ρ_0 = initial atmospheric density at $R = R_0$
ρ_1 = final atmospheric density at $R = R_1$
$\tilde{\rho}$ = density coefficient

Introduction

THERE are applications where it is desirable to place a group of satellites in prescribed low circular orbits. Orbit decay of such satellites is influenced primarily by atmospheric drag (Refs. 1, 2, and their references). However, when it is desired to maintain the group of satellites at fixed relative distances, the effects of small differences in ballistic coefficient also become a problem of interest. This note presents the results of an investigation on the drift distance between two satellites caused by a small difference in ballistic coefficient which might be due to differences in weight, frontal area, geometry, and surface roughness. Other perturbing mechanisms, such as the earth's oblateness, variation of earth's gravity field, the gravity effects of the sun and moon, and magnetic field have secondary effects which apply almost equally to each satellite and will, therefore, be neglected. The present analysis is also limited to circular orbits at altitudes less than 400 miles where atmospheric drag has the dominating effect on orbit decay, and where the effects of solar radiation pressure are also negligible.

Using high-speed computers to solve this long-term decay problem from the equations of motion is costly. A numerical solution could accumulate, after a few orbits of calculation, errors of the same magnitude as the drift distance. Therefore, a closed-form solution is desirable. Billik,[1] Parsons,[2] Henry,[3] and Perkins[4] have obtained closed-form solutions for satellite lifetimes. Recently, Zee[5] has analyzed satellite trajectories under the influence of air drag and has obtained an approximate solution for anomaly angle. He obtained u, the ratio of perigee focal radius of original elliptical orbit to radial distance from the center of attraction to the satellite by assuming constant h, ratio of the angular momentum. He then substituted these results in a nondimensional equation of motion and expanded it into a series. Neglecting

Presented as Preprint 64-477 at the 1st AIAA Annual Meeting, Washington, D. C., June 29–July 2, 1964; revision received January 6, 1965. This paper is based on original research work performed while the author was Staff Scientist, Aerospace Division, Boeing Company. (Any views expressed in this paper are those of the author. They should not be interpreted as reflecting the views of The Rand Corporation or the official opinion or policy of any of its governmental or private research sponsors. Papers are reproduced by The Rand Corporation as a courtesy to members of its staff.)

* Research Engineer, Aero-Astronautics Department. Associate Fellow Member AIAA.

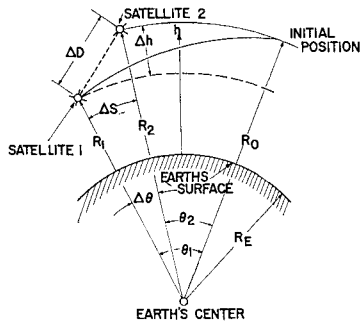

Fig. 1 Circular orbit geometry.

all the high-order terms, keeping only the first two terms in the equation, and applying the asymptotic method developed by Bogoluiboff and Mitropolsky, he obtained approximate solutions. This note presents an exact closed-form solution for satellite anomaly as a function of altitude by assuming the density to be an exponential function of altitude. Better accuracy can be obtained by summing the anomaly over a number of density subarcs. Results and simplified solutions are presented.

Method of Analysis

The equations of motion of a satellite traveling in a circular earth orbit[1,2] are given as follows (see Fig. 1):

$$\dot{h} = (-\rho/\beta)g_E^{3/2}R_E R^{1/2} \tag{1}$$

$$\dot{\theta} = g_E^{1/2}R_E R^{-3/2} \tag{2}$$

The initial conditions at $t = 0$ are

$$\theta = 0 \qquad R = R_0 \qquad \text{or} \qquad h = h_0 = R_0 - R_E$$

The density ρ has been taken historically as an exponential function of altitude,[1-6] namely,

$$\rho = \bar{\rho}e^{-\gamma h} \tag{3}$$

where $\bar{\rho}$ and γ are constant matching coefficients. A fit to the U. S. Standard Atmosphere, 1962, made between 50 to 400 miles at various intervals, is tabulated in Table 1. The differences between exponential fits for subarcs of ρ vs h and the U. S. Standard Atmosphere, 1962, are very small (<3%) and could be further reduced by using smaller intervals. Substituting Eq. (3) into Eq. (1)

$$\dot{h} = (-\bar{\rho}/\beta)g_E^{3/2}R_E e^{-\gamma h}R^{1/2} \tag{4}$$

But by definition

$$\ddot{\theta} = (\dot{h})^2\frac{d^2\theta}{dh^2} + \ddot{h}\frac{d\theta}{dh} \tag{5}$$

Table 1 U. S. Standard Atmosphere 1962, matching coefficients

Altitude, h, nm	Reciprocal of scale height, γ 1/nm	Coefficient, $\bar{\rho}$ slugs/ft^3
50–55	3.328×10^{-1}	6.131×10^{-2}
55–60	2.923×10^{-1}	6.527×10^{-3}
60–65	2.531×10^{-1}	6.102×10^{-4}
65–70	2.169×10^{-1}	5.798×10^{-5}
70–75	1.497×10^{-1}	5.290×10^{-7}
75–80	1.167×10^{-1}	4.435×10^{-8}
80–90	8.017×10^{-2}	2.324×10^{-9}
90–100	5.868×10^{-2}	3.409×10^{-10}
100–120	4.860×10^{-2}	1.232×10^{-10}
120–140	4.171×10^{-2}	5.398×10^{-11}
140–160	3.758×10^{-2}	3.036×10^{-11}
160–180	3.386×10^{-2}	1.673×10^{-11}
180–200	3.142×10^{-2}	1.081×10^{-11}
200–250	2.759×10^{-2}	4.928×10^{-12}
250–300	2.380×10^{-2}	1.902×10^{-12}
300–350	2.135×10^{-2}	9.150×10^{-13}
350–382	2.007×10^{-2}	5.866×10^{-13}

Differentiation of Eqs. (4) and (2) with respect to t yields

$$\ddot{h} = \frac{\rho}{\beta}g_E^{3/2}R_E R^{1/2}(\gamma)\dot{h} - \frac{\rho}{2\beta}g_E^{3/2}R_E R^{-1/2}\dot{h} \tag{6}$$

$$\ddot{\theta} = -\tfrac{3}{2}g_E^{1/2}R_E R^{-5/2}\dot{h} \tag{7}$$

Substituting Eqs. (4) and (6) into Eq. (5) and equating Eq. (5) with Eq. (7) yields

$$\frac{d^2\theta}{d^2R} + \left(\frac{1}{2R} - \gamma\right)\frac{d\theta}{dR} = \frac{3\beta e^{\gamma(R-R_E)}}{2\bar{\rho}g_E R^3} \tag{8}$$

where $R = R_E + h$. The general solution of Eq. (8) is

$$\theta = C_1\int R^{-1/2}e^{\gamma R}dR + C_2 - \frac{2A}{3\bar{\rho}}e^{-\gamma R}E_R^{-3/2} \times \int R^{-1/2}e^{\gamma R}dR - \frac{A}{\bar{\rho}e^{\gamma R_E}}\int R^{-5/2}\int R^{-1/2}e^{\gamma R}(dR)^2 \tag{9}$$

where $A = 3\beta/2g_E$ and

$$\int R^{-1/2}e^{\gamma R}dR = 2e^{\gamma R}R^{1/2}\sum_{\nu=0}^{\infty}\frac{(-2\gamma R)^2}{(1;2;\nu+1)} \times (1;2;\nu+1) = (1+2\nu)!/2(\nu!)$$

Here, C_1 and C_2 are constants of integration to be determined from the initial conditions.

Differentiating Eq. (9) with respect to t

$$\dot{\theta} = (-\rho/\beta)g_E^{3/2}R_E[C_1 - \tfrac{2}{3}(A/\bar{\rho})e^{-\gamma R_E}R^{-3/2}]e^{\gamma R} \tag{10}$$

Applying the second initial condition to Eq. (10) yields

$$C_1 = 0 \tag{11}$$

From the remaining initial condition, one obtains

$$C_2 = \frac{2}{3}\left[\frac{A}{\bar{\rho}}e^{-\gamma R_E}R^{-3/2}\int R^{-1/2}e^{\gamma R}dR\right]_{R=R_0} + \left[\frac{A}{\bar{\rho}}e^{-\gamma R_E}\int R^{-5/2}\int R^{-1/2}e^{\gamma R}(dR)^2\right]_{R=R_0} \tag{12}$$

Therefore, the general solution Eq. (9) can be rewritten as

$$\theta = \frac{-\beta}{\bar{\rho}_0 g_E}e^{-\gamma_0 R_E}[R^{-3/2}\int R^{-1/2}e^{\gamma R}dR\Big]_{R=R_0}^{R=R} - \frac{3\beta}{2\bar{\rho}_0 g_E}e^{-\gamma_0 R_E}\int_{R_0}^{R}R^{-5/2}\int R^{-1/2}e^{\gamma R}(dR)^2 \tag{13}$$

Integrating Eq. (1) gives

$$t = \frac{\beta e^{-\gamma R_E}}{\bar{\rho}_0 g_E^{3/2}R_E}\int_{R_0}^{R}R^{-1/2}e^{\gamma R}dR \tag{14}$$

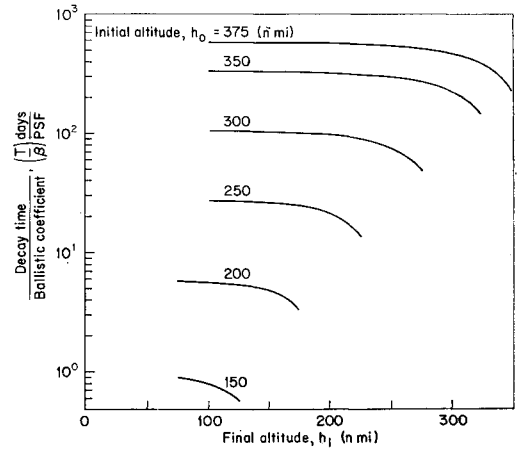

Fig. 2 Earth satellite lifetime in days for circular orbits.

If after a given time t satellite no. 1, which has a ballistic coefficient β_1, reaches an altitude of h_1, while the no. 2 satellite with $\beta_2 = \beta_1 + \Delta\beta$ reaches an altitude h_2 as shown in Fig. 1, then equating the times for these two cases of Eq. (14) gives

$$\beta_1 = \Delta\beta \frac{\int_{R_0}^{R_2} R^{-1/2} e^{\gamma_0 R} dR}{\int_{R_2}^{R_1} R^{-1/2} e^{\gamma_0 R} dR} \tag{15}$$

where $R_1 = R_E + h_1$, $R_2 = R_E + h_2$, and $\Delta\beta$ is very small.

The difference in angle traveled also can be expressed as

$$\Delta\theta = \theta_1 - \theta_2$$

$$= \frac{-\Delta\beta}{\bar{\rho}_0 g_E} e^{-\gamma_0 R_E} \frac{\int_{R_0}^{R_2} R^{-1/2} e^{\gamma_0 R} dR}{\int_{R_2}^{R_1} R^{-1/2} e^{\gamma_0 R} dR} \left\{ \left[R^{-3/2} \int R^{-1/2} e^{\gamma R} dR \right]_{R_2}^{R_1} + \frac{3}{2} \int_{R_2}^{R_1} R^{-5/2} \int R^{-1/2} e^{\gamma R} (dR)^2 \right\} + \frac{\Delta\beta}{\bar{\rho}_0 g_E} e^{-\gamma_0 R_E} \times \left\{ \left[R^{-3/2} \int R^{-3/2} e^{\gamma R} dR \right]_{R_0}^{R_2} + \frac{3}{2} \int_{R_0}^{R_2} R^{-5/2} \int R^{-1/2} e^{\gamma R} (dR)^2 \right\} \tag{16}$$

Using the cosine law, the total drift distance ΔD between two satellites, due to a small difference in ballistic coefficient $\Delta\beta$, can then be written approximately as

$$\frac{\Delta D}{\Delta\beta} = \frac{[R_1^2 + (R_1 + \Delta h)^2 - 2R_1(R_1 + \Delta h)\cos(\Delta\theta)]^{1/2}}{\Delta\beta} \cong \frac{2^{1/2} R_1 [1 - \cos(\Delta\theta)]^{1/2}}{\Delta\beta} \tag{17}$$

where $\Delta\theta$ is given in Eq. (16). As mentioned earlier, better accuracy can be obtained by summing the flight time and anomaly over a number of density subarcs. This allows $\bar{\rho}$ and γ to assume those values that give the best atmospheric fit at smaller intervals of altitude. Equations (13) and (14) can then be written as

$$\theta \cong \frac{-\beta}{g_E} \sum_{j=0}^{n} \frac{e^{-\gamma_i R_E}}{\bar{\rho}_j} \left[R^{-3/2} \int R^{-1/2} e^{\gamma_i R} dR \right]_{R_j}^{R_{j+}} - \frac{3\beta}{2g_E} \sum_{j=0}^{n} \frac{e^{-\gamma_i R_E}}{\bar{\rho}_j} \int_{Rj}^{R_{j+1}} R^{-1/2} e^{\gamma_i R} dR \tag{18}$$

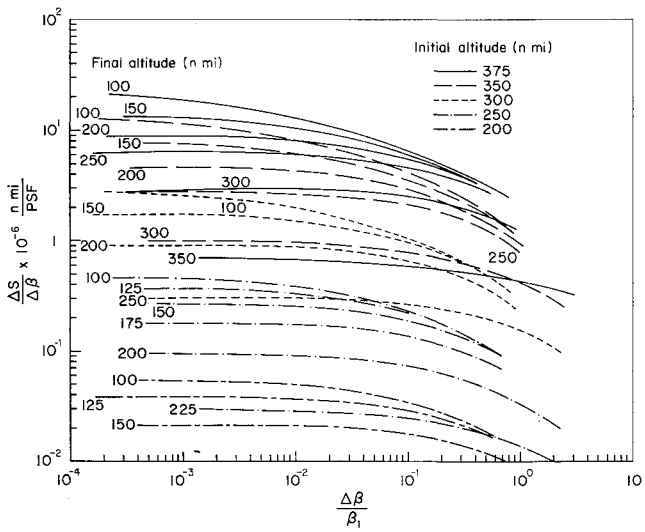

Fig. 3 Influences of difference in ballistic coefficient on circumferential drift distance.

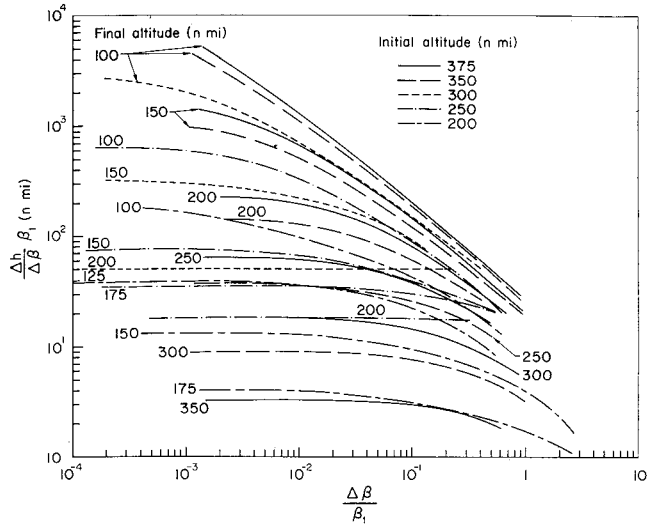

Fig. 4 Influences of difference in ballistic coefficient on drift altitude.

and

$$t \cong \frac{\beta}{g_E^{3/2} R_E} \sum_{j=0}^{n} \frac{e^{-\gamma_i R_E}}{\bar{\rho}_j} \int_{R_j}^{R_{j+1}} R^{-1/2} e^{\gamma_i R} dR \tag{19}$$

where n corresponds to the number of subdivisions of density. The integrands appearing in Eqs. (18) and (19) must be evaluated numerically. However, if density subdivisions are very small, the terms $R^{-1/2}$ and $R^{-5/2}$ may be considered to be constants $R_j^{-1/2}$ and $R_j^{-5/2}$, respectively. This approximation was also used by Parsons.[2] Then the integrands in Eqs. (18) and (19) can be readily evaluated, or Eqs. (13) and (14) become, respectively,

$$\theta \cong -\beta[R^{-3/2}\rho^{-1} - R_0^{-3/2}\rho_0^{-1}]/g_E R_0^{1/2}\gamma_0 - 3\beta[\rho^{-1} - \rho_0^{-1}]/2g_E R_0^3 \gamma_0^2 \tag{20}$$

and

$$t \cong -\beta[\rho^{-1} - \rho_0^{-1}]/[g_E^{3/2} R_E \gamma_0 R_0^{1/2}] \tag{21}$$

Equations (15) and (16) can also be rewritten, respectively, as

$$\beta_1 = -\Delta\beta[\rho_2^{-1} - \rho_0^{-1}]/[\rho_1^{-1} - \rho_2^{-1}] \tag{22}$$

$$\frac{\Delta\theta}{\Delta\beta} \cong \frac{\rho_0\rho_2(R_1^{-3/2} - R_2^{-3/2}) - \rho_2^2(R_1^{-3/2} - R_0^{-3/2}) + \rho_1\rho_2(R_2^{-3/2} - R_0^{-3/2})}{-g_E R_0^{1/2}\gamma_0\rho_0\rho_2(\rho_2 - \rho_1)} \tag{23}$$

where $\Delta\beta$ is the small difference in ballistic coefficient between two satellites.

Numerical Results and Discussion

The earth satellite lifetime in days for circular orbits can be obtained directly from Eqs. (18) and (19). The simplified equations are given in Eqs. (20) and (21). Since other forms of the solutions have been derived,[3-6] it was not the purpose of this note to obtain Eqs. (18) and (19). However, the final results computed from Eqs. (18) and (19) by using the U. S. Standard Atmosphere, 1962, are plotted in Fig. 2. Figure 3 shows the effects of differences in ballistic coefficient on satellite circumferential drift distance for various initial altitudes. For instance, if h_0 and h_1 are taken as 375 and 350 n miles, respectively, if the reference satellite has $\beta_1 = 1$, and the difference between ballistic coefficients between two satellites is only $\Delta\beta = 0.00155$, a decay time of 235 days can be obtained from Fig. 2. The corresponding circumferential drift distance $\Delta S \cong 690\ n$ miles can be obtained from Fig. 3. This is a very small number in comparison

with the traveled distance which is over 10^8 n miles in 235 days. The drift distance can be positive or negative, depending on the ballistic coefficient. If a satellite ballistic coefficient is smaller than that of the reference satellite β_1, the circumferential drift distance will be positive and vice versa.

The effects of $\Delta\beta$ on drift altitude are shown in Fig. 4 for various initial and final altitudes. For the conditions given in the example in the previous paragraph, the corresponding drift altitude is about $\Delta h \cong 0.0065\ n$ miles.

References

[1] Billik, B., "Survey of current literature on satellite lifetime," ARS J. **32**, 1641–1650 (1962).

[2] Parsons, W. D., "Orbit decay characteristics due to drag," ARS J. **32**, 1876–1881 (1962).

[3] Henry, I., "Lifetimes of artificial satellites of the earth," Jet Propulsion **27**, 21–24 (January 1957).

[4] Perkins, F., "An analytical solution for flight time of satellite in eccentric and circular orbits," Astronaut. Acta **4**, 113–134 (1958).

[5] Zee, C.-H., "Trajectories of satellites under the influence of air drag," AIAA Preprint 63-392 (August 1963).

[6] Billik, B., "The lifetime of an earth satellite," Aerospace Corp., TN-594-1105-1 (December 1960).

Forces Due to Gaseous Slot Jet Boundary-Layer Interaction

HARVEY DERSHIN*

General Dynamics/Pomona, Pomona, Calif.

Nomenclature

d_j = jet slot width
F = normal force per unit width
I = specific impulse based on jet mass flow
K = Crocco-Lees profile parameter
k = mixing-rate coefficient
L = distance from leading edge to jet
M = Mach number
$\dot{m}$ = mass flow rate
P = pressure
R_e = Reynolds number
u = longitudinal velocity
x = distance along plate
y = distance normal to plate
γ = ratio of specific heats
ρ = density

Subscripts

j = jet exit
$0j$ = jet stagnation
P = plateau
∞ = freestream

Introduction

THE use of reaction jets for control of high-altitude aerodynamic vehicles or space vehicles is well known. It is also of interest to consider using this control method at all altitudes. The advantages are 1) replacement of structural control surfaces eliminating a possible aerodynamic heating problem and offering the possibility of a weight saving, and 2) omission of system overlap for a vehicle with wide altitude range. The main question, however, refers to the effective control forces. This note offers an approximate solution to one portion of this problem, i.e., the control forces due to the interaction between a supersonic boundary layer and a slot-type (i.e., two-dimensional) gaseous jet issuing normal to the vehicle surface. The results are presented as a ratio of effective aerodynamic control force to jet-reaction force. Comparisons are made with experimental data.

Received September 2, 1964; revision received November 30, 1964. The author would like to thank E. E. Zukowski and F. W. Spaid for their useful comments.

* Staff Scientist. Member AIAA.

Analysis

The flow model under consideration is shown in Fig. 1, and the following assumptions are made:

1) The upstream boundary layer is either all laminar or all turbulent.

2) Separation has occurred upstream of the jet.

3) The majority of the upstream separated flow (i.e., after separation and before recompression) can be characterized as a constant pressure mixing region.

4) The jet Mach number is ≥ 1.0, and the jet profiles are slug type.

5) The region downstream of the jet is sufficiently short so that the net effective side force due to overexpansion is small and no mixing takes place.

6) The entire flow is isoenergetic.

Then, assuming a negligibly thin boundary layer at (0, 0′), a momentum balance over the volume (0, 0′, 2, 3, 4, 1, 0) yields†

$$\dot{m}_{34}u_{34} - \Delta\dot{m}_p u_p = P_p y_{12} - P_{34}y_{34} \tag{1}$$

The quantity $\Delta\dot{m}_p$ represents the mass influx through plane (0′-2). And, as a first approximation, $\Delta\dot{m}_p u_p$ is assumed to be totally imposed on the jet. The parameter $\Delta\dot{m}_p$ can be determined by approximating the Crocco-Lees mixing-rate coefficient[1] by

$$k = (\Delta\dot{m}_p/\Delta x_s)/\rho_p u_p \tag{2}$$

Then, assuming an average (k) over the mixing region, it is seen that the length of the mixing region (Δx_s) is given by

$$\Delta x_s = [P_{34}y_{34}(1 + \gamma_j M_{34}^2) - P_p y_{12}]/\gamma_\infty P_p M_p^2 k \tag{3}$$

For the downstream regions, mass conservation of the jet flow can be written as

$$P_{0j}d_j M_j\{1 + [(\gamma - 1)/2]M_j^2\} \exp[(1 + \gamma_j)/2(1 - \gamma_j)] = P_{34}y_{34}M_{34}\{1 + [(\gamma_j - 1)/2]\, M_{34}^2\}^{1/2} \tag{4}$$

Substituting (4) into (3)

$$\Delta x_s/d_j = (P_{0j}M_j\{1 + [(\gamma - 1)/2]M_j^2\} \exp[(1 + \gamma_j)/2(1 - \gamma_j)]\bar{B})/\gamma_\infty P_p M_p^2 k \tag{5}$$

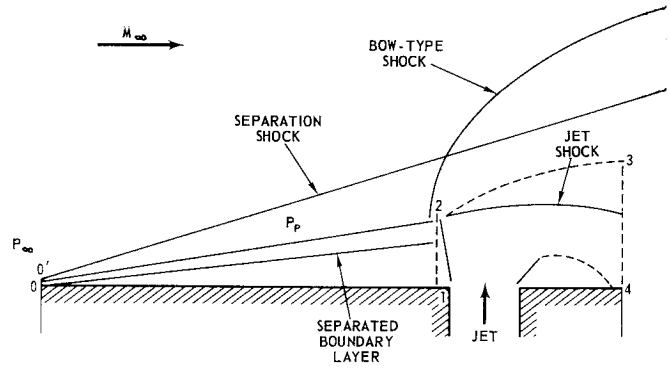

Fig. 1 Jet interaction model.

† Where the force on the downstream jet contact surface and the momentum due to jet curvature are assumed to be equal and mutually balancing.